Journal of Basic and Environmental Sciences

ISSN
Online:2356-6388
Print:2536-9202

Research Paper Open Access

Biosynthesis of silver nanoparticles using aqueous *Euphorbia paralias* extract and their anticancer activity

Walaa A. Ismail[a], Abdel-Naby M. Salem[a], Mostafa M.H. Khalil[*,a]

[a] Chemistry Department, Faculty of Science, Ain Shams University, Abbassia, 11566, Cairo, Egypt.

Corresponding author: Mostafa M. H. Khalil (**e-mail:** khalil62@yahoo.com ; Mostafa_khalil@sci.asu.edu.eg)

Abstract

In this study silver nanoparticles (AgNPs) were synthesized using water extract of the aerial parts of *Euphorbia paralias* (E. paralias) as reducing and stabilizing agents. Various experimental parameters, including sample pH, temperature, reaction time, extract composition, and metal salt concentration, were examined for their effects on the size and morphology of the AgNPs. The synthesized silver nanoparticles (AgNPs) were characterized using UV-Vis spectroscopy, FTIR, X-ray diffraction (XRD), transmission electron microscopy (TEM), and thermal gravimetry. The formation of AgNPs began within 3 minutes and progressively increased over time for two hours. The synthesized nanoparticles were predominantly spherical, with an average size varying between 15 and 35 nm. Bio-fabricated AgNPs have more significant anticancer activity against HepG2, MCF-7, and HCT-116 with IC50 = 20.3 ± 1.8, 30.4 ± 3.8, and 45.2 ± 2.5 µg/ml respectively. The anticancer activity of the aqueous extract of *Euphorbia paralias* with IC50 > 500 µg/ml indicates that AgNPs exhibit synergistic effects as the diverse range of phytochemicals present in plant extracts, combined with the small size and large surface area of AgNPs, allows for maximum adsorption of these capping agents onto their surfaces and improves the therapeutic performance of phyto- AgNPs in anticancer activity.

Keywords: Keywords: *Euphorbia paralias*, Bio-fabricated AgNPs; HepG2; MCF-7; HCT-116.

1. Introduction

In 2020, more than nineteen million new cancer cases and ten million cancer-related deaths were recorded worldwide (**WHO-Cancer Report-2020**). Breast cancer accounted for the highest proportion of diagnoses (11.7%), followed by lung cancer (11.6%), colorectal cancer (10%), and prostate cancer (7.3%). Moreover, expert projections suggest that by 2040, the number of cancer cases will rise to 24.8 million, representing a 47% increase compared to 2020. (**Sung et al. 2021**). Cancer treatment is very costly, requiring expensive facilities and drugs and chemotherapy medications can damage healthy cells in addition to killing rapidly proliferating cancer cells, resulting in adverse effects that spread throughout the body. To provide safe and dependable treatment, new methods are required to develop anticancer medicines that are effective but have fewer side effects and are less toxic in the clinic. Given this outlook, the development of new treatments and drugs will be challenging unless governments allocate a greater share of resources to cancer care. Insufficient funding could hinder access to high-quality treatment and care (**Voda and Bostan, 2018**). New cancer therapies typically focus on developing more effective drugs while minimizing the side effects associated with anticancer treatments. However, the plant kingdom remains largely unexplored; many anticancer drugs, such as those derived from *Euphorbia*, originate from plants. Euphorbia species are commonly utilized in traditional medicine for addressing stomach, liver, and uterine cancer-related ailments. Additionally, these species have been applied in the management of asthma conditions. Numerous other species have been employed to treat skin disorders, gonorrhea, migraine headaches, intestinal parasites, as well as warts and calluses (**Ben Jannet et al. 2017**).

Euphorbia paralias L is one of the most common *Euphorbia* species growing in Egypt (**Abdelgaleil et al., 2001**). Chemical constituents of *Euphorbia paralias L* species have been investigated previously and showed that phenolic compounds, steroids, terpenes, hydrocarbons, and alkaloids are various phytochemicals detected in the genus Euphorbia. These phytochemicals have potential anticancer and antioxidant (**Youssef et al. 2024**). Miloud and Senussi examined the antimicrobial activity of leaf extracts from two *Euphorbia* species, namely *Euphorbia paralias* and *Melilotus sulcatus*, against four bacterial species (*Staphylococcus aureus*, *Pseudomonas*

aeruginosa, *Escherichia coli*, and *Klebsiella* sp.) and two fungal species (*Aspergillus niger* and *Aspergillus flavus*) (**Miloud and Senussi, 2021**). Euphorbia paralias polar extract showed the presence of many chemical compounds such as flavanol (as catechin, myricetin and quercetin, Quercetin-3-O-b-Darabinopyranoside), flavonoids (as chalcone), the monoterpenoids (as linalool), and the polyphenol (as ellagic acid) (**Youssef et al. 2024**). The extracts demonstrated greater effectiveness against bacterial species than fungi at the tested concentration (100 mg/mL). Methanolic extracts of the selected plants exhibited significant antimicrobial potential against all tested microorganisms, whereas aqueous extracts showed no activity against the fungal species tested. Furthermore, beyond its established targets in mycobacterial cells, Q3G has been demonstrated to effectively inhibit the glutamine synthetase enzyme, a promising target for developing new drugs for TB therapy (**Safwat et al. 2018**).

Recently, botanical-based synthesis of Ag has attracted increasing interest due to its cost-effectiveness, simplicity, and environmentally friendly synthesis methods (**Yadav et al. 2025, Stozhko et al. 2024, Rashidi 2024, Jamil et al. 2024, Vadakkan et al. 2024**, **Alex et al. 2024**). The chemical reduction of Ag+ ions to form Ag^{o} nanoparticles is usually performed using physicochemical techniques such as sodium citrate ($Na_3C_6H_5O_7$) **(Chen et al. 2020**), polyol synthesis (**Zeroual et al. 2020**), biologic process (**Zevallos Torres et al. 2021**), electrochemical techniques (**Thuc et al. 2016**), and surfactant-assisted synthesis (**Molina Torres et al 2019** These conventional methods are often toxic, unstable, expensive, time-intensive, and detrimental to the environment.The necessity to use a benign, l ess hazardous, ecofriendly, and biocompatibl e process for developing AgNPs of various dimensions and shapes has increased (**Aziz et al., 2020**). Although biological approaches have limitations, such as limited control over nanoparticle size, shape, and crystalline structure, they are widely regarded as safe, practical, cost-effective, and environmentally sustainable (**Yousaf et al. 2020**). Generally, NP size and morphological features are greatly influenced by the experimental parameters, including sample pH, temperature, reaction time, extract type, and metal salt interaction with reducing chemicals **(Khalil et al. 2014**). Researchers are interested in synthesizing AgNPs using plant extract because it is a quick, environmentally friendly, non-toxic, economically viable, and one-step biosynthetic approach. Plant metabolites are typically employed as liquid extracts of seeds, fruits, flowers, tree bark, leaves, peels, and rhizomes.

In the present study, water extract of *Euphorbia paralias* was used for the synthesis of AgNPs, and the characteristics of the bio-fabricated silver nanostructures were analyzed using UV–vis, Fourier transform infrared FTIR, TEM, EDX, and XRD. The cytotoxic and anti-cancer activities of the extract and the bio-fabricated AgNPs against mammalian cell lines: HepG-2 cells (human Hepatocellular carcinoma), MCF-7 cells (human Breast carcinoma) and HCT-116 (human Colon carcinoma) were evaluated.

2. Experimental

2.1. Chemicals and Extract Preparation

The chemicals used for the synthesis were of analytical grade. Silver nitrate ($AgNO_3$, 99.7%) was purchased from Sigma-Aldrich Chemicals. *E. paralias* plant was harvested in April in 2022 from the region of Ageba area, Mersa-Mattruh, on the Mediterranean coast of Egypt. The aerial parts were air-dried, grounded to a fine powder, and kept being used for various analyses.

2.2 Preparation of *E. paralias* aerial parts extract.

An ***E. paralias*** aerial parts extract was prepared by boiling 0.50 g of dried, finely ground aerial parts of *E. paralias* in 50 mL of deionized water for 20 minutes. The mixture was then filtered, and the volume was adjusted to 50 mL with deionized water. Fresh extract was prepared for each experiment.

2-3 Synthesis of AgNPs using *E. paralias* aqueous extract:

Stock solution of $AgNO_3$ (10^{-2} M) was prepared by dissolving a 0.17 gm of $AgNO_3$ in 100 mL flask with deionized water. At room temperature, 1 mL of $AgNO_3$ (10^{-2} M) was mixed with (0.1- 1 ml) of *E. paralias* extract and complete to 10 mL. The reduction process was followed by the change in the color of the solution and UV–visible spectra of the samples were measured after 2h. The highest absorbance was found for the ratio of 1 mL $AgNO_3$ to 1 mL of the extract. Using this ratio the effect of reaction time was followed by UV–visible spectroscopy to optimize the reaction time. Also, the effect of pH of the solution on the reduction process was done at this ratio in a 10 mL flask and the pH was adjusted using 0.05 M HNO_3 and 0.1 M NaOH. The effect of temperature was measured using 1mL $AgNO_3$ to 1 mL of the extract, and the samples' absorbance was measured at the temperature range from 20-90 ^{0}C.

2-4 Characterization of Ag Nanoparticles

The process of reduction of Ag^+ ions to form AgNPs in solution was followed by measuring the UV-Vis spectra of the reaction mixtures on a wavelength range of 200–800 nm using a Shimadzu UV-2600

UV-Vis spectrophotometer with quartz cuvettes of 10 mm optical path length, resolution 2 nm. All measurements were conducted against a reference sample containing water, which served as the solvent in the synthesis. The size and morphology of the nanoparticles were analyzed through transmission electron microscopy (TEM), and the images were obtained using a JEOL-1200JEM microscope. For TEM analysis, a drop of the synthesized AgNPs colloid was placed onto carbon-coated copper grids and allowed to air-dry. XRD analysis of the AgNPs was performed using a Shimadzu XRD-6000 diffractometer operating at 40 kV and 20 mA, with Cu Kα radiation (λ = 1.54 Å). Fourier-transform infrared (FTIR) spectroscopy was performed to identify the functional groups potentially involved in nanoparticle formation. The analysis was conducted both before and after the synthesis of nanoparticles, using samples of the powdered aerial parts and the synthesized nanoparticle (NP) powder. The bio-reduced silver nanoparticles (AgNPs) were centrifuged at 10,000 rpm for 15 minutes, after which the samples were dried, ground with potassium bromide (KBr), and analyzed using a Nicolet 6700 FTIR spectrometer to obtain the FTIR spectra of the capped nanoparticles. Thermogravimetric analysis was performed at a heating rate of 10 °C/min using a Shimadzu DT-50 thermal analyzer to determine the quantity of capping phytochemicals present on the AgNPs.

2.5. Evaluation of Cytotoxic Effects of *E. paralis and capped AgNPs*

The cytotoxicity assay was conducted using the microculture MTT method with minor modifications **(Kawase et al., 2003, Soliman et al. 2018).** Cell viability and inhibition were calculated using the formula: % viability = (A_t/A_c) x100, where A_t = Absorbance of the test sample and A_c = Absorbance of the control sample. The 50% inhibitory concentration (IC50) was determined from graphical plots of the dose-response curves for each concentration.

3. Results and Discussion

3.1. Preparation of AgNPs using *E. paralis* extract and characterization

For monitoring the formation and stability of silver nanoparticles, the Uv-Vis spectra of the synthesized silver nanoparticles were recorded against water as reference. Figure 1 shows the absorption spectra of the UV–visible spectra of silver nanoparticle formation using constant $AgNO_3$ concentration (10^{-2}M) with different extract volumes (0.1 – 1.0 mL) at room temperature. The AgNPs display changing in color from pale yellow to brown, indicating the formation of silver nanoparticles; the color arises due to the

excitation of Surface Plasmon Resonance (SPR) of the AgNPs. The surface plasmon resonance (SPR) of silver nanoparticles (AgNPs) was observed at 430 nm, attributed to the excitation of surface plasmon vibrations. With the addition of 0.1-1.0 ml of *E. paralis* aerial parts extract, the surface plasmon intensity increased with the increase of the extract concentration indicating more AgNPs formation. On the other hand, increasing the volume of the extract from 1 mL to 2 mL the absorbance very slightly increased due to the end of the reduction signifying that 1-2 mL was adequate to reduce most of the silver ions to nanosilver. Further increase in the volume of the extract led to a slight decrease in the absorbance (Fig. 1). The optimum volume of 1mL extract was used in the subsequent experiments.

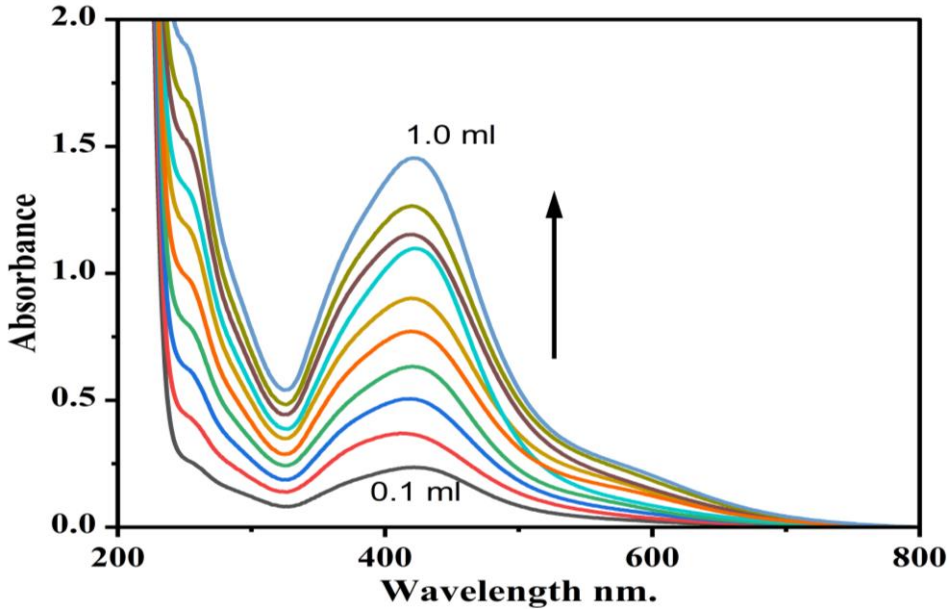

Figure (1): The absorption spectra of AgNps as a function of *E. paralis* aerial parts extract concentration.

The bio-produced AgNPs was further characterized by employing Transmission Electron Microscopy (TEM). The TEM images confirm the formation of the AgNPs which were spherical with an average size of 15 nm and 35nm demonstrated a range of different morphologies with irregular contours when 0.3 mL of extract was used in the synthesis, Fig. 2(a). When 1 mL of extract was used, the AgNPs had an average size of 18 nm (Fig. 2b), and their size decreased further when 2 mL of extract was used (Fig. 2c). It can be concluded that the size of AgNps is getting smaller with increasing the extract concentration which works as a reducing and capping agent to enhance nucleation and reduce the agglomeration process of the nanoparticles. Similar studies showed that a comparatively higher extract ratio is responsible for the synthesis of symmetrical nanoparticles (**Sosa, 2003**).

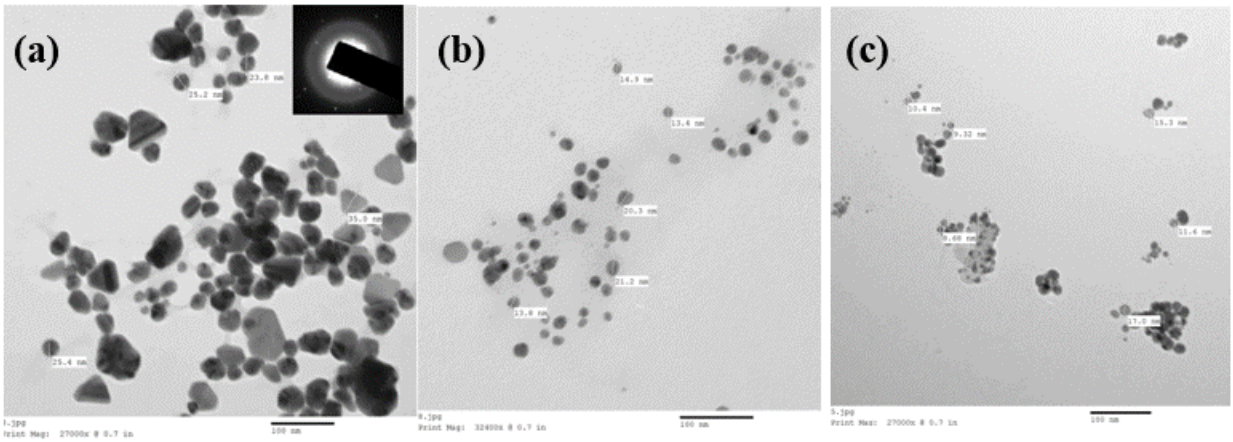

Figure (2): Effect of the *E. paralis* aerial parts extract concentration on the size and shape of the AgNPs. (a) TEM image of AgNPs using 0.3 ml *E. paralis* extract (b) TEM image measured using 1 ml *E. paralis* extract; (c) shape of AgNPs formed at 2 ml of extract.

3.2 Impact of contact time

The effect of contact time between Ag^+ ions and the extract were investigated at room temperature to determine the reaction rate and the duration required to complete the reduction process. Figure 3 illustrates that the formation of AgNPs began within 3 minutes and progressively increased over time. The absorption band showed minimal changes after two hours, indicating the complete reduction of Ag^+ to Ag^0. It is worth noting that previous studies reported a reduction period for silver ions ranging from 24 to 48 hours (**Sosa, 2003, Khalil et al. 2017**) or longer time as one week (**Lin et al. 2010, Dipankar and Murugan, 2012, Bindhu and Umadevi, 2013**).

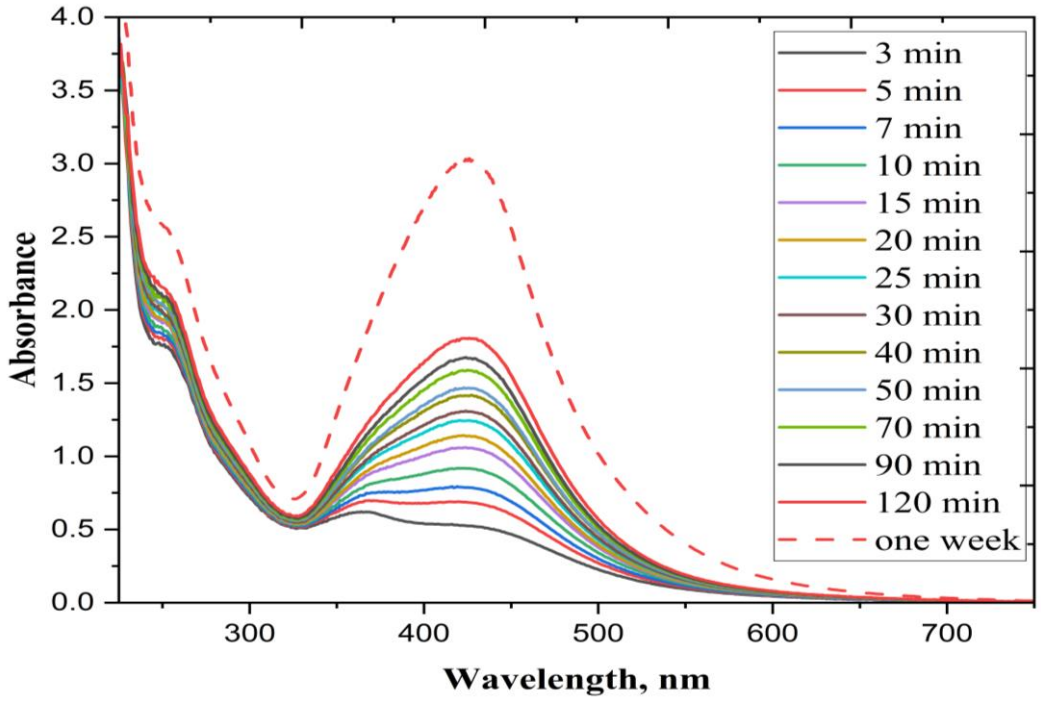

Figure (3): Effect of contact time on AgNPs formation (1 mL *E. paralis* aerial parts extract and constant (10^{-2} M) $AgNO_3$).

3. 3. Effect of extract pH

The pH of the extract used in nanoparticle biosynthesis is a crucial factor influencing the size, shape, and composition of the resulting nanoparticles. **(Khalil et al. 2014)**. Using UV-Vis spectroscopy and TEM analysis, the effect of the pH of *E. paralis* aerial parts extract solution on the biosynthesis of Ag nanoparticles was examined across a pH range of 3 to 11, Figures 4. It can be seen from Fig. 4, that at pH 3, AgNPs show lower and broader absorbance like the extract, and no clear band for the surface plasmon resonance of AgNPs was observed. Furthermore, a blue shift in the absorbance maximum was observed from 444 nm at pH 4 to 412 nm at pH 9.6; the plasmon resonance band became sharper and the absorption peak intensity increased gradually with an increase in pH, suggesting that the reduction rate of silver ions increases with the increase in pH. This behavior may be due to the ionization of phenolic, flavanol catechin, myricetin quercetin, and flavonoids compounds in the extract of *E. paralis* (**Priya et al. 2016, Traiwatcharanon et al. 2015**) that can increase the rate of AgNPs formation. Upon increasing the pH higher than 9.6, a solid residue starts to form, maybe due to the precipitation of Ag_2O. In many previous studies, using the basic medium is necessary to obtain AgNPs.and found that on increasing the pH, rate of the reaction increased along with decrease in reaction time especially when $pH > 7$ for both green assisted and chemically synthesized AgNPs. This behaviour of pH on the growth of nanoparticles can be attributed to its capability to modify the charge of bio-compounds present in the leaf extract [Verma and Mehata, 2016]. Additionally, optimal value of pH for synthesis of AgNPs attributed to high absorbance peak value, low λ_{max} (wavelength value for maximum absorbance/LSPR peak position) and high population of smaller sized NPs were found to be pH 12 and pH 10 for biosynthesized and chemically synthesized AgNPs respectively [Ajitha et al. 2015]. The AgNPs synthesized in an acidic medium (pH 2-5) were unstable and precipitated within 24 hours, whereas those prepared at pH 9 remained stable for one week. So, the optimum pH used in the synthesis of AgNPs was 9.

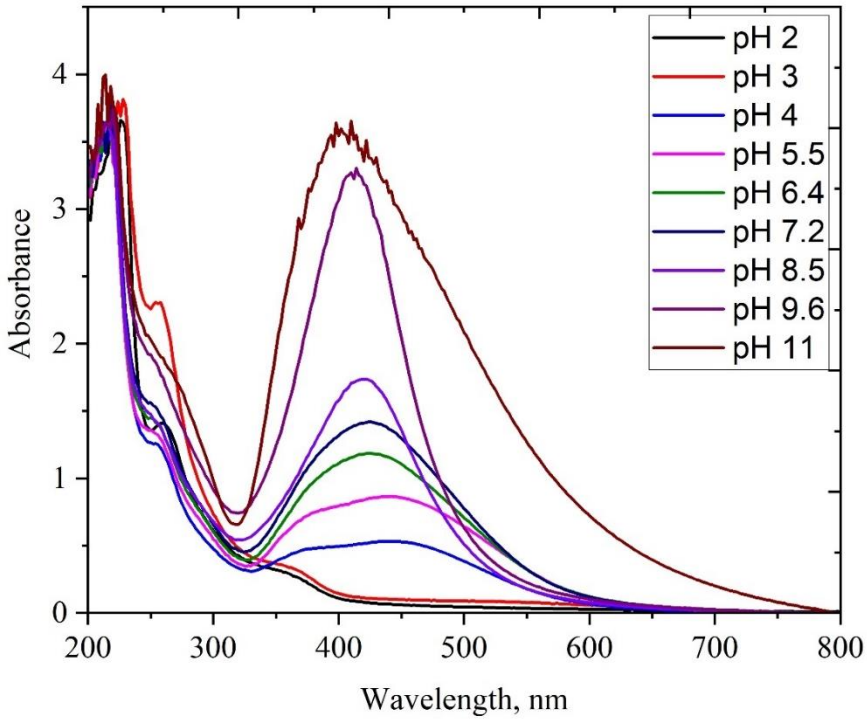

Figure (4): Effect of pH on silver nanoparticles synthesis by *E. paralis* aerial parts extract.

3.4 Effect of Reaction Temperature

Temperature significantly influences the synthesis of silver nanoparticles (AgNPs), affecting their size, shape, stability, and overall yield. Higher temperatures generally increase the reduction rate of silver ions (Ag^{+}) to metallic silver (Ag^{0}), promoting faster nucleation and growth of nanoparticles. This leads to smaller and more uniform nanoparticles due to rapid nucleation over slower growth processes. On the other hand, elevated temperatures can destabilize certain stabilizing agents, potentially leading to the aggregation of nanoparticles. As seen in Fig. 5, as the temperature increased from 20 to 90 ^{0}C, at pH 6, the absorption spectra of AgNPs increased with blue shift from 425 nm to 411 nm indicating that smaller size formation increased with temperature and the formed AgNPs are stable.

3.5 FTIR spectra

FTIR spectroscopy was employed to identify the potential functional groups of biomolecules in the *E. paralis* aqueous extract that could be responsible for the bio-reduction and coating of AgNPs. The FTIR spectrum of the extract displayed a broad band at 3402 cm^{-1}, which is attributed to the OH groups present in the biomolecules. The band at 1662 cm^{-1} is assigned to the stretching vibration of the carbonyl group (C=O), and (C=C) potentially indicating the presence of keto groups in flavonoids, Fig. 6. The band at 1280 cm^{-1} (probably related

to C-O of polyols),. Besides the bands previously described, there was another band encountered at 748 cm^{-1} due to aromatic ring vibration. These assignments consisted of the isolated flavonoids that might be present in the constituent of *E. paralis* extract, (Fig. 7).

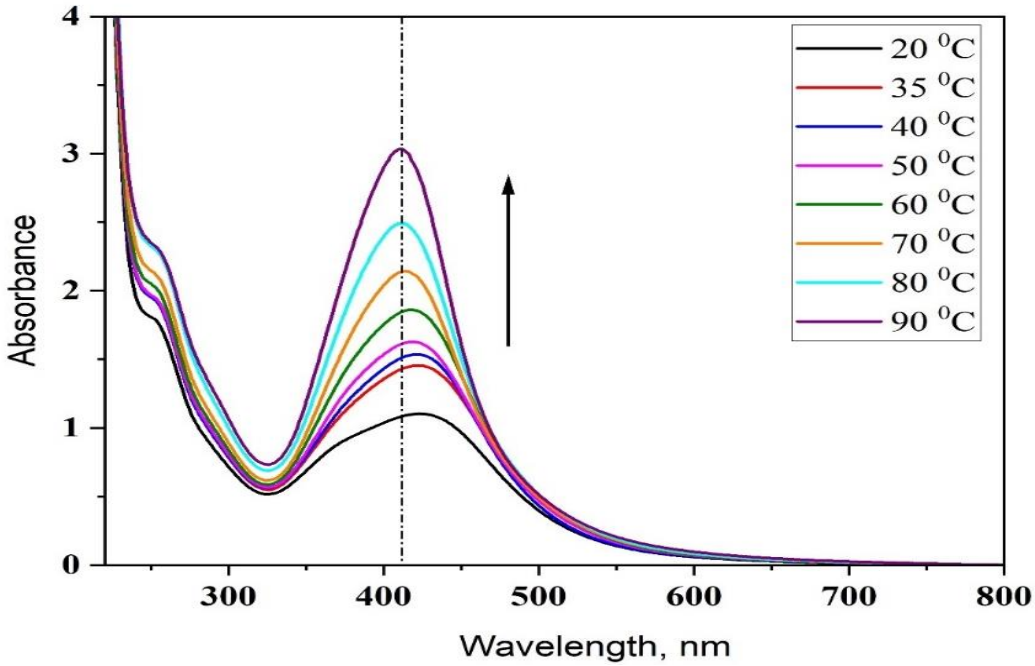

Figure (5): Effect of temperature on silver nanoparticles synthesis by *E. paralis*.

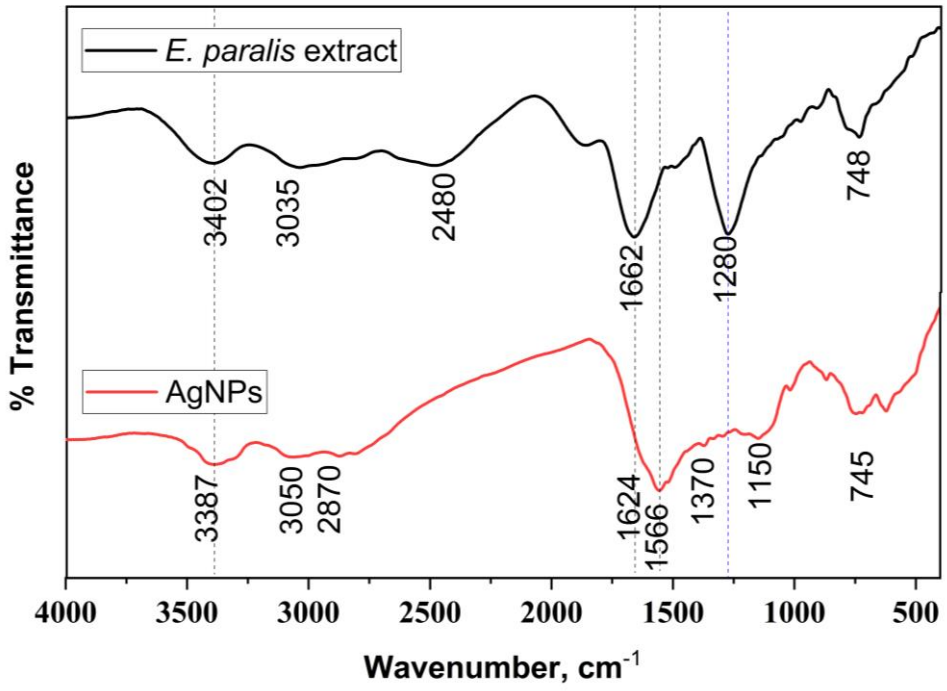

Figure (6): FTIR spectra of E. paralis and E. paralis capped AgNps.

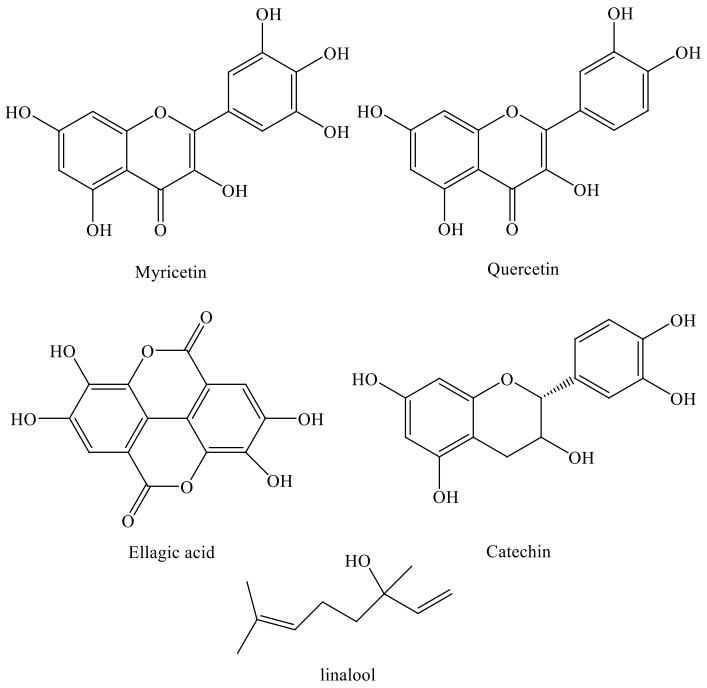

Figure (7): Compounds present in *E. paralis*.

3.7. Thermal gravimetric analysis

The TGA plot of the capped AgNPs prepared using 2 ml *E. paralis* extract (Fig. 8 showed a relentless weight loss in the temperature range of 160–700 ^{0}C. The final weight of the nanopowder due to the desorption of bioorganic compounds on the AgNPs was 27.5%. This means that AgNPs can adsorb large amounts of extract compounds on their surface and be used as drug carriers for cancer treatment. Similar DTA spectrum of AgNPs synthesized by *Streptomyces aqueous extract* obtained by Paterlini et al. 2021 [Paterlini]. They attributed the loss of weight to the desorption of organic compounds from the surface of the NPs with a residual mass of 20% would correspond to the AgNPs.

3.8 X-ray diffraction

The XRD pattern of the phyto-synthesized AgNPs prepared using the *E. paralis* extract is shown in Figure 9. The XRD results confirmed that the AgNPs correspond to the crystalline face-centered cubic phase of silver. Four distinct Bragg reflections observed at 2θ = 38.035° (111), 44.76° (200), 64.46° (220), and 77.39 ° (311) match those reported in the standard powder diffraction card of JCPDS, silver file No. 04-0783. The data revealed the crystalline nature of AgNPs (**Shameli et al 2010**).

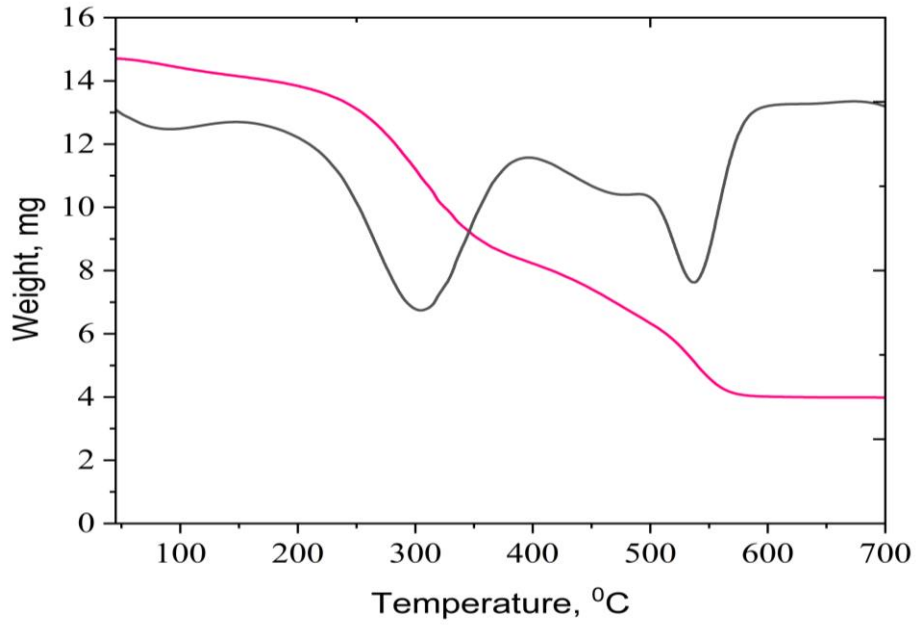

Figure (8): TGA of capped Ag NPs prepared using E. ***paralis*** extract.

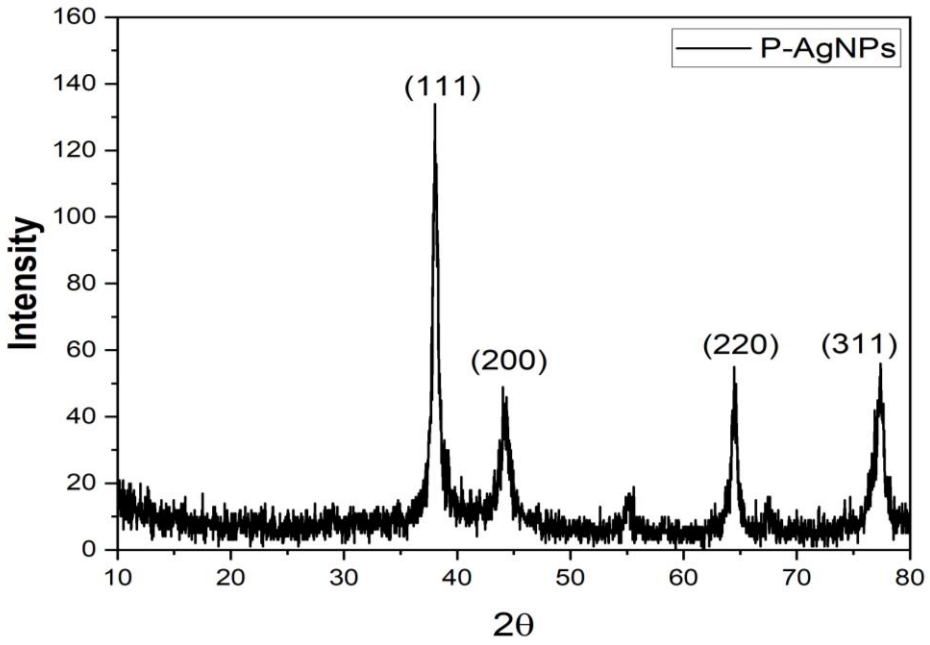

Figure (9): XRD of capped AgNPs prepared using E. ***paralis*** extract at the conditions (pH =9, temp. = 90 ^{0}C, reaction time = 15 min).

3.9 In vitro cytotoxicity activity

E. paralias contains various phytochemicals that may have anticancer and antioxidant activities. The antioxidant activity was identified by the ability of the extract to reduce Ag^+ to Ag^0 to produce AgNPs. As shown from the thermogravimetric analysis, high extract concentrations are present and capped the AgNPs due to the smaller size of the nanoparticles and high surface area. One

can use this fact to utilize the capped AgNPs to treat cancer in at relatively small quantity of capped AgNPs.

In vitro cytotoxicity assays are widely used to assess chemicals such as cancer therapeutics, pharmaceuticals, biomaterials, natural toxins, antimicrobial agents, and industrial chemicals because they are fast and cost-efficient. These assays measure the concentration of a substance that causes damage to cellular components and structures, providing quantitative or biochemical data that can be extrapolated to simulate in vitro biological pathways. (**Irena, 2005**). The *in vitro* anticancer activity of the synthesized nanoparticles was assessed against human cancer cell lines, including hepatocellular carcinoma (HepG2), MCF-7 cells (human breast carcinoma), and HCT-116 cells (human colon carcinoma), using the MTT assay (**Denizot and Lang 1986**). Doxorubicin hydrochloride (IC50: 1.2 µg/mL), a highly potent anticancer agent, was used as the reference drug in this study. The correlation between drug concentrations and cell viability was analyzed to determine the IC50 value, which indicates the concentration needed to reduce cell viability by 50%. The results are presented in Table 1 and Figure 11. According to the data in Table 1, the aqueous extract of *E. paralias* is cytocompatible, while the AgNps has cytotoxic activity with IC_{50} of 20.3 ± 1.8, 30.4 ± 3.8, and 45.2 ± 2.5 µg/ml, against HepG2, MCF-7, and HCT-116, respectively that is considered to be a promising cytotoxic agent. It is worth noting that the IC50 of 74.6 ± 15.6 was obtained for the extract in methanol against MCF-7, supporting that the methanol extract would have more concentrated bioorganic compounds than the water extract (**Youssef et al. 2024**).

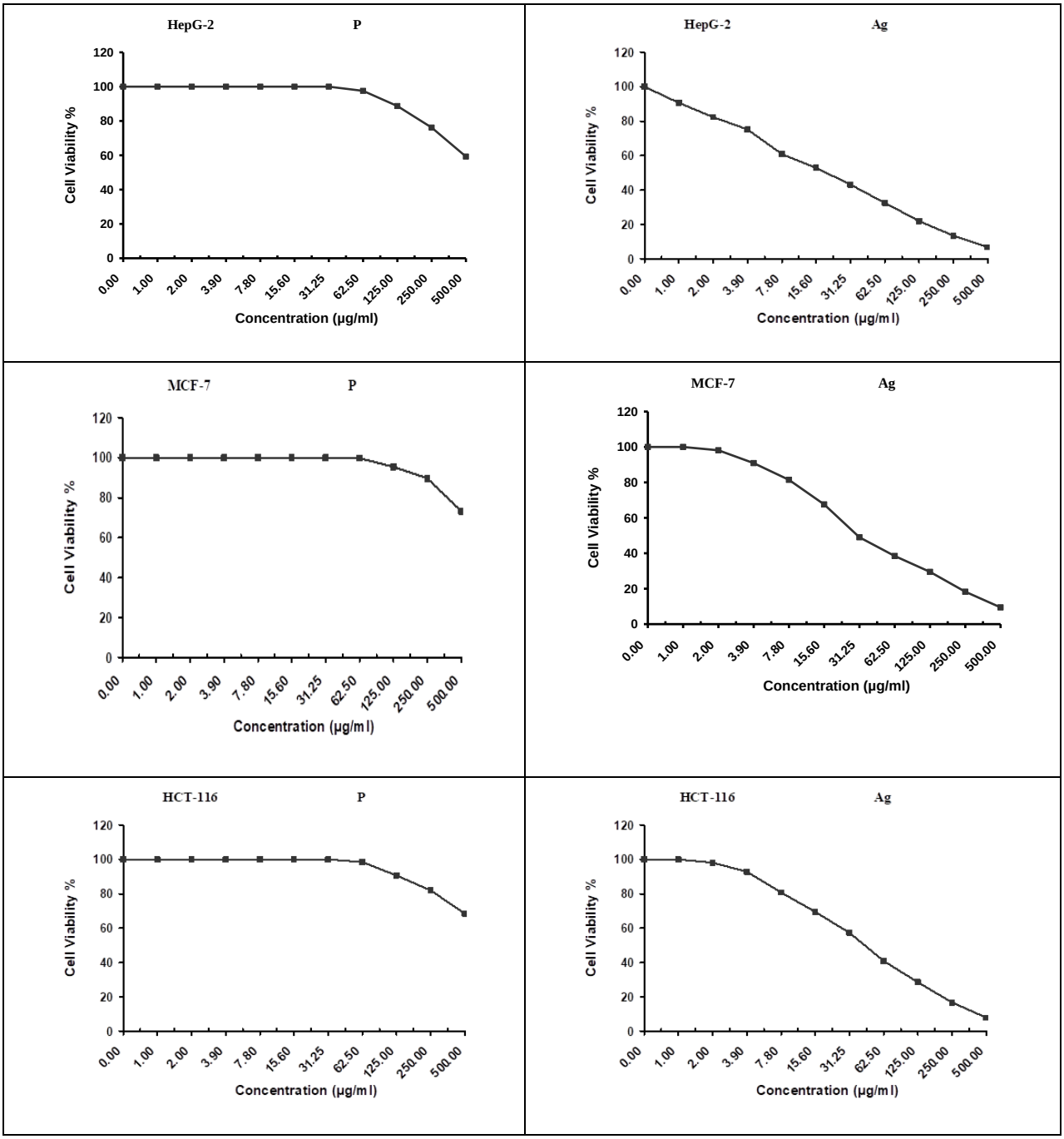

Figure (10): Cell viability of *E. paralias* aqueous extract and AgNPs on different cancer cell lines.

Tabel 1

The IC50 of *E. paralias* aqueous extract and AgNPs values of cancer cell lines

Item/ IC50	HepG-2	MCF-7	HCT-116
Euphorbia paralias	>500	> 500	> 500
P-AgNPs	20.3 ± 1.8 µg/ml	30.4 ± 3.8 µg/ml	45.2 ± 2.5 µg/ml

4. Conclusion

In conclusion, silver nanoparticles (AgNPs) were successfully synthesized at room temperature through an eco-friendly approach, utilizing *Euphorbia paralias* extract as both the reducing and stabilizing agent. The synthesis parameters, such as extract concentration, reaction time, and pH, were thoroughly investigated. The optimum conditions for the synthesis of AgNPs in this study was as following: pH 9, contact time 60 min and at 90 ^{0}C. The IC50 of the synthesized AgNPs capped with biomolecules from the extract were evaluated for cytotoxic activity against HepG-2, MCF-7, and HCT-116 cell lines, The results indicated cytotoxic activity of AgNPs capped with E. paralias was higher than the aqueous extract. In the future work, the aqueous E. paralias extract will be used to synthesize Ag-Au NPs as alloy and study their activity as antimicrobial and anticancer drugs. The use of plant phytochemical and its aqueous solution for the synthesis of AgNPs as green method that do not use toxic chemicals in the synthesis protocols to avoid adverse effects in medical applications.

5. References

Abdelgaleil, S. A. M., Kassem, S. M. I., Doe, M., Baba, M., & Nakatani, M. (2001). Diterpenoids from Euphorbia paralias. *Phytochemistry*, *58*(7): 1135–1139.

Ajitha B, Reddy YA, Reddy PS (2015). Enhanced antimicrobial activity of silver nanoparticles with controlled particle size by pH variation. Powder Technol.269:110–7

Alex, A.M., Subburaman, S., Chauhan, S., Ahuja V., Abdi G. & Tarighat M. A. (2024) Green synthesis of silver nanoparticle prepared with *Ocimum* species and assessment of anticancer potential. *Sci Rep* 14:11707.

Aziz, A. T., Alshehri, M. A., Alanazi, N. A., Panneerselvam, C., Trivedi, S., Maggi, F., Sut, S., & Dall'Acqua, S. (2020). Phytochemical analysis of rhazya stricta extract and its use in fabrication of silver nanoparticles effective against Mosquito Vectors and microbial pathogens. *Science of The Total Environment*, *700*: 134443.

Ben Jannet, S., Hymery, N., Bourgou, S., Jdey, A., Lachaal, M., Magné, C., & Ksouri, R. (2017). Antioxidant and selective anticancer activities of two Euphorbia species in human acute myeloid leukemia. *Biomedicine & Pharmacotherapy*, *90*: 375–385.

Bindhu, M.R., Umadevi, M., (2013). Synthesis of monodispersed silver nanoparticles using Hibiscus cannabinus leaf extract and its antimicrobial activity. Spectrochimica Acta Part A 101: 184–190

Chen, J. E., Wang, Q., Shull, K. R., & Richards, J. J. (2020). Control over electroless plating of silver on silica nanoparticles with sodium citrate. *Journal of Colloid and Interface Science*, *576*: 376–384.

Das, U., Daimari, N.K., Biswas, R. Mazumder *N*., (2024*)* Elucidating impact of solvent and pH in synthesizing

silver nanoparticles via green and chemical route. Discov Appl Sci 6: 320

Denizot F. and Lang R., (1986) Rapid colorimetric assay for cell growth and survival. Modifications to the tetrazolium dye procedure giving improved sensitivity and reliability, *Journal of Immunological Methods*. **89**: 271–277

Dipankar, C., Murugan, S., (2012). The green synthesis, characterization and evaluation of the biological activities of silver nanoparticles synthesized from Iresine herbstii leaf aqueous extracts. Colloids Surf., B 98: 112–119.

Irena K. (2005) Synthetic and natural coumarins as cytotoxic agents. *Curr Med Chem-Anti-Cancer Agents*. 5:29-46.

Kawase, M., Motohashi, N., Satoh, K., Sakagami, H., Nakashima, H., Tani, S., Shirataki, Y., Kurihara, T., Spengler, G., Wolfard, K., & Molnár, J. (2003). Biological activity of persimmon (*diospyros kaki*) peel extracts. *Phytotherapy Research*, *17*(5): 495–500.

Khalil, M. M. H., Ismail, E. H., El-Baghdady, K. Z., & Mohamed, D. (2014). Green synthesis of silver nanoparticles using olive leaf extract and its antibacterial activity. *Arabian Journal of Chemistry*, *7*(6): 1131–1139.

Khalil, M.M.H, Sabry D.Y., Mahdy, H., (2017) Green synthesis of silver, gold and silver-gold nanoparticles: Characterization, antimicrobial activity and cytotoxicity Journal of scientific Research in Science. 34: 553–574.

Lin, L., Wang, W., Huang, J., Li Q., Sun, D., Yang, X., Wang, H., He, N., Wang, Y., (2010). Nature factory of silver nanowires: plant-mediated synthesis using broth of Cassia fistula leaf. Chem. Eng. J. 162: 852–858.

Miloud, M. M., & Senussi, N. A. (2021). Antimicrobial activity of leaf extracts of Euphorbia paralias L. and melilotus sulcatus DESF. against some pathogenic microorganisms. Current Botany, 12: 10–15.

Molina Torres, M. A., Pachón Gómez, E. M., Fernández, M. A., Veglia, A. V., & Pacioni, N. L. (2019). Role of a cystine-based Gemini surfactant ligand in the synthesis of catalytic active silver nanoparticles. *Journal of Molecular Liquids*, *284*, 110–116.

Jamil, Y.M. S. Al-Hakimi, A. N. ; Al-Maydama H. M. A., Almahwiti G. Y., Qasem A., Saleh S. M. (2024) Optimum Green Synthesis, Characterization, and AntibacterialActivity of Silver Nanoparticles Prepared from an Extract of Aloe fleurentinorum, International Journal of Chemical Engineering 2024: 2804165.

Rashidi, M.A., Falahi, S., Dehghan S. F., Ebrahimzadeh H., Ghaneialvar H.& Zendehdel R. **(2024)** Green synthesis of silver nanoparticles by *Smyrnium cordifolium* plant and its application for colorimetric detection of ammonia. *Sci Rep* **14:** 24161.

Paterlini P., Rodríguez C., Ledesma A., Pereyra J., Costa J. S. D., Álvarez A., Romero C. M. (2021) Characterization of biosynthesized silver nanoparticles from Streptomyces aqueous extract and evaluation of surface-capping proteins involved in the process, Nano-Structures & Nano-Objects, 26:100755

Priya R S, Geetha D and Ramesh P S (2016) Antioxidant activity of chemically synthesized AgNPs and biosynthesized Pongamia pinnate leaf extract mediated AgNPs - a comparative study, Ecotoxicol. Environ. Saf. 134: 308–18.

Safwat, N. A., Kashef, M. T., Aziz, R. K., Amer, K. F., & Ramadan, M. A. (2018). Quercetin 3-O-glucoside recovered from the wild Egyptian Sahara plant, Euphorbia

paralias L., inhibits glutamine synthetase and has antimycobacterial activity. Tuberculosis, 108: 106–113.

Shameli, K., Ahmad, M.B., Yunus, W.M.Z.W., Ibrahim, N.A., (2010). Synthesis and characterization of silver/talc nanocomposites using the wet chemical reduction method. Int. J. Nanomed. 5: 743–751.

Soliman, N, A. , Ismail E. H., Abd El-Moaty H. I., Sabry, D. Y. and Khalil M. M.H, (2018) Anti-Helicobacter pylori, anti-diabetic and cytotoxicity activity of biosynthesized gold nanoparticles using *Moricandia nitens* water extract,. Egypt. J. Chem. 61: 691-703.

Sosa, I.O., Noguez, C., Barrera, R.G., (2003). Optical properties of metal nanoparticles with arbitrary shapes. J. Phys. Chem. B 107: 6269–6275.

Stozhko, N.; Tarasov, A.; Tamoshenko, V.; Bukharinova, M.; Khamzina, E.; Kolotygina, V. (2024) Green Silver Nanoparticles: Plant-Extract-Mediated Synthesis, Optical and Electrochemical Properties. Physchem , 4*:* 402-419.

Sung, H., Ferlay, J., Siegel, R. L., Laversanne, M., Soerjomataram, I., Jemal, A., & Bray, F. (2021). Global cancer statistics 2020: Globocan estimates of incidence and mortality worldwide for 36 cancers in 185 countries. *CA: A Cancer Journal for Clinicians*, *71*(3), 209–249.

Thuc, D. T., Huy, T. Q., Hoang, L. H., Tien, B. C., Van Chung, P., Thuy, N. T., & Le, A.-T. (2016). Green synthesis of colloidal silver nanoparticles through electrochemical method and their antibacterial activity. *Materials Letters*, *181*, 173–177.

Traiwatcharanon P., Timsorn K., Wongchoosuk C., (2015) Effect of pH on the Green Synthesis of Silver Nanoparticles through Reduction with *Pistiastratiotes L.* Extract, Advanced Materials Research 1131: 223-226

Vadakkan K., Rumjit N. P., Ngangbam A. K., Vijayanand S., Nedumpillil, N. K. (2024) Novel advancements in the sustainable green synthesis approach of silver nanoparticles (AgNPs) for antibacterial therapeutic applications, Coordination Chemistry Reviews, 499: 215528.

Verma A, Mehata MS. **(2016)** Controllable synthesis of silver nanoparticles using Neem leaves and their antimicrobial activity. J Radiat Res Appl Sci. 9:109–15.

Voda, A.I.; Bostan, I. (2018) Public Health Care Financing and the Costs of Cancer Care: A Cross-National Analysis. *Cancers*, 10: 117.

World Health Organization (WHO) 2020. WHO-Cancer Report-2020-Global Profile; World Health Organization (WHO): Geneva, Switzerland,.

Yadav V. K., Gupta R., Assiri A.A., Uddin J., Ishaqui A. A., Kumar P., Orayj K.M., Tahira S., Patel A. & Choudhary N. (2025) Role of Nanotechnology in Ischemic Stroke: Advancements in Targeted Therapies and Diagnostics for Enhanced Clinical Outcomes. *Journal of Functional Biomaterials* 16: 1-8.

Yousaf, H., Mehmood, A., Ahmad, K. S., & Raffi, M. (2020). Green synthesis of silver nanoparticles and their applications as an alternative antibacterial and antioxidant agents. Materials Science and Engineering: *C*, *112*: 110901.

Youssef A, Althneibat T, Maaty D, Al Hujran T, Al-Saraireh Y (2024) Bioactive compounds and profiling of anticancer and antioxidant activities of

Euphorbia paralias L. family Euphorbiaceae. J Pharm Pharmacogn Res 12(4): 786–799.

Zeroual, S., Estellé, P., Cabaleiro, D., Vigolo, B., Emo, M., Halim, W., & Ouaskit, S. (2020). Ethylene glycol based silver nanoparticles synthesized by Polyol Process: Characterization and Thermophysical Profile. *Journal of Molecular Liquids*, *310*: 113229.

Zevallos Torres, L. A., Woiciechowski, A. L., Oliveira de Andrade Tanobe, V., Zandoná Filho, A., Alves de Freitas, R., Noseda, M. D., Saito Szameitat, E., Faulds, C., Coutinho, P., Bertrand, E., & Soccol, C. R. (2021). Lignin from oil palm empty fruit bunches: Characterization, biological activities and application in green synthesis of silver nanoparticles. *International Journal of Biological Macromolecules*, *167*: 1499–1507.